

## Mössbauer-effect study of ferromagnetic $DO_3$ -structured iron-aluminum-silicon alloys

Mou-Ching Lin, R. G. Barnes, and D. R. Torgeson

Ames Laboratory-U.S. Department of Energy and Department of Physics, Iowa State University, Ames, Iowa 50011

(Received 30 March 1981)

Mössbauer-effect spectroscopy has been used to measure the temperature dependence of the  $^{57}\text{Fe}$  effective magnetic hyperfine field  $H_{\text{eff}}$  and isomer shift  $\delta$  across the entire  $\text{Fe}_3\text{Al}_x\text{Si}_{1-x}$  system ( $0 \leq x \leq 1$ ) from 77 K to the Curie temperature, the latter also being determined from these measurements. The observed dependence of  $H_{\text{eff}}$  and  $\delta$  on Al concentration can be qualitatively understood in terms of the calculated band structure of  $\text{Fe}_3\text{Si}$ . The changes in  $H_{\text{eff}}$  and  $\delta$  at the  $B$  sites with increasing Al concentration are due primarily to a decrease in the number of spin-up electrons at these sites, whereas the changes in  $H_{\text{eff}}$  and  $\delta$  at the  $A, C$  sites result primarily from a decrease in the number of spin-down electrons at these sites.

### I. INTRODUCTION

An extensive, technologically significant class of ferromagnetic alloys is formed by iron, aluminum, and silicon crystallizing in the  $DO_3$ -structure-type binary phase,  $\text{Fe}_3\text{Al}_x\text{Si}_{1-x}$  ( $0 \leq x \leq 1$ ). The unit cell of the  $DO_3$  structure is shown in Fig. 1. It is comprised of four interpenetrating face-centered-cubic (fcc) sublattices conventionally designated  $A, B, C,$  and  $D$ . All  $D$  sites are occupied by Si(Al) atoms, and all  $A, B,$  and  $C$  sites by Fe atoms. The iron atoms on  $B$  sites,  $\text{Fe}(B)$ , have all iron nearest neighbors, NN, whereas iron on  $A$  and  $C$  sites,  $\text{Fe}(A)$  and  $\text{Fe}(C)$ , have four Fe and four Si(Al) nearest neighbors.

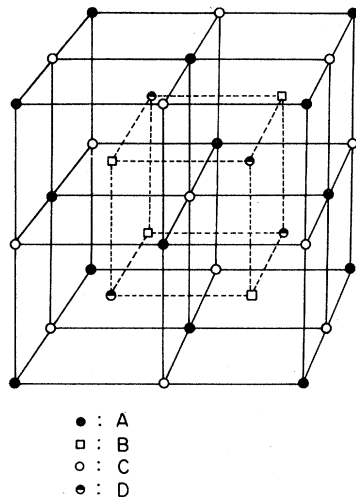


FIG. 1 Unit cell of the  $DO_3$  structure. Type  $A, C,$  and  $B$  sites are occupied by iron atoms in perfectly ordered  $\text{Fe}_3\text{Al}_x\text{Si}_{1-x}$  alloys and type- $D$  sites by aluminum and silicon atoms.

Effective magnetic hyperfine fields and local magnetic moments have been shown to be sensitive indicators of the local atomic environment in alloys. Neutron diffraction measurements have shown that different magnetic moments exist on the  $B$  and  $A, C$  sites in both  $\text{Fe}_3\text{Al}$  and  $\text{Fe}_3\text{Si}$ ,<sup>1-3</sup> i.e., 2.4 and  $1.2\mu_B$  per site, respectively, for the  $B$  and  $A, C$  sites in  $\text{Fe}_3\text{Si}$  and 2.18 and  $1.50\mu_B$  per site, respectively, in  $\text{Fe}_3\text{Al}$ . Similarly, Mössbauer-effect measurements have shown the effective magnetic hyperfine fields,  $H_{\text{eff}}$ , to be different for the  $B$  and  $A, C$  sites in both  $\text{Fe}_3\text{Al}$  and  $\text{Fe}_3\text{Si}$ .<sup>4</sup> In a model proposed by Niculescu *et al.*<sup>5</sup> the magnetic moments depend critically on the number of Fe atoms in the first NN shell, yielding reasonable explanations for the behavior observed in both the  $\text{Fe}_{3-x}\text{Mn}_x\text{Si}$  ( $0 \leq x \leq 1.6$ ) and the  $\text{Fe}_{3-x}\text{V}_x\text{Si}$  ( $0 \leq x \leq 1$ ) systems. This model suggests that the dominant interactions in  $\text{Fe}_3\text{Si}$  and its alloys are short range. The major contribution to  $H_{\text{eff}}$  from polarization of the  $4s$  electrons arises from interactions with the moments in the first NN shell. More distant neighbors contribute to changes in spin polarization by perturbing the first NN moment. Haydock and You<sup>6</sup> employed a local environment approach based on Stoner theory and a linear combination of atomic orbitals (LCAO) model to calculate the magnetic moments in ordered  $\text{Fe}_3\text{Al}$  and obtained results in good agreement with experiment. In this model they emphasized that the reduction of the moment on the  $A, C$  sites does not result simply from the presence of fewer Fe atoms in the first NN shell, but rather from more Al atoms.

In a simple model, Fe has eight outer ( $d + s + p$ ) electrons, Si has four ( $s + p$ ) electrons, Al has three ( $s + p$ ) electrons. As  $x$  increases from 0 to 1 in the  $\text{Fe}_3\text{Al}_x\text{Si}_{1-x}$  system the total number of ( $s + p + d$ ) electrons per formula unit decreases from 7.0 to 6.75, and at the same time the lattice constant, measured by Cowdery and Kayser,<sup>7</sup> increases from 5.6533 to

5.7934 Å. The NMR spin-echo technique was used by Niculescu *et al.*<sup>8</sup> to measure  $H_{\text{eff}}$  of  $^{57}\text{Fe}$  at 1.3 K in  $\text{Fe}_3\text{Al}_x\text{Si}_{1-x}$  ( $0 \leq x \leq 0.25$ ). These results indicate that  $H_{\text{eff}}$  decreases monotonically at both Fe(*A*), Fe(*C*), and Fe(*B*) sites as  $x$  increases.

The nonmagnetic energy band structure of  $\text{Fe}_3\text{Si}$  has been calculated by Switendick.<sup>9</sup> Based on these results, a rigid level, spin-polarized model yields both charge transfer and different magnetic moments at the two sites, *B* and *A*, *C*, and explains satisfactorily the observed moments, moment changes, and differing preferential site occupations of transition-metal solutes to the left and to the right of iron in the periodic table. Specifically, the effects of substituting Mn for Fe in the  $\text{Fe}_3\text{Si}$  lattice to give  $\text{Fe}_2\text{MnSi}$  are (1) to remove electrons from *A*, *C* sites, (2) to reduce charge transfer from *B* to *A*, *C* sites, and (3) to decrease the exchange splitting. Treating the  $\text{Fe}_3\text{Al}_x\text{Si}_{1-x}$  system as one in which Al substitutes for Si in the  $\text{Fe}_3\text{Si}$  lattice, we anticipate that similar effects will occur. Since  $^{57}\text{Fe}$  Mössbauer spectroscopy provides information on the magnitude and polarization of *s* electron wave functions at the  $^{57}\text{Fe}$  nuclei, and since these in turn depend strongly on the local environment of the Fe atom, any effects due to the replacement of Si atoms by Al atoms should be revealed in the Mössbauer spectra and their temperature dependence. This paper reports  $^{57}\text{Fe}$  Mössbauer-effect measurements across the entire  $\text{Fe}_3\text{Al}_x\text{Si}_{1-x}$  system ( $0 \leq x \leq 1$ ) from liquid nitrogen (77 K) to the Curie temperature. The band-structure calculation of Switendick is used to explain the observed variations in  $H_{\text{eff}}$  and in the isomer shift as functions of  $x$ . The temperature dependence of  $H_{\text{eff}}$  and the measured Curie temperatures provide further insight into the strength of the moment coupling interaction. The temperature dependence of  $H_{\text{eff}}$  is discussed in terms of a mean-field theory which combines the itinerant and localized characters of the moments. However, quantitative fits of Brillouin-function type behavior to the experimental data could not be achieved.

## II. EXPERIMENTAL

All of the alloy samples investigated were prepared and furnished by Professor F. X. Kayser's group in the Ames Laboratory. Details of the preparation and annealing of the powder samples may be found in Ref. 7.

The Mössbauer source was a commercial 10.9-mCi  $^{57}\text{Co}$  in a copper matrix having a source linewidth of 0.099 mm/sec. Spectra were obtained with a TMC 1024 channel analyzer coupled with a Ranger Electronics spectrometer operated in constant acceleration mode. To calibrate and check the system, the spectrum of an enriched  $^{57}\text{Fe}$  absorber foil was recorded

about every third run. The estimated statistical uncertainty for all spectra is less than 0.35%.

For measurements between room temperature and the Curie temperature a Ricor MF-2 vacuum furnace was used in a vertical geometry with the source drive mounted above the furnace. Samples were spread on boron nitride (BN) holders (disks) and covered with a second BN disk to ensure temperature homogeneity over the entire sample. Temperatures were measured with a Chromel/Alumel thermocouple whose junction was in contact with the BN holder and were servo controlled to within  $\pm 0.1$  K. The thermocouple calibration was based on measurements of the temperature dependence of  $H_{\text{eff}}$  of Fe foil samples. Curie temperatures were determined to within  $\pm 2$  K by monitoring directly the collapse of the spectrum into a single line.

For the low-temperature measurements the samples were clamped to a massive copper rod connected to the liquid-nitrogen reservoir of a stainless-steel cryostat with Be windows.

## III. EXPERIMENTAL RESULTS

The Mössbauer spectra of all the alloy samples were fit with two sets of six Lorentzian lines. The accuracy of the fit, as measured by  $\chi^2$ , was typically 1 to  $1\frac{1}{2}$  times the expected value, probably reflecting the fact that the experimental spectrum lines were not strictly Lorentzian. With the exception of  $\text{Fe}_3\text{Si}$ , spectrum lines in all spectra were broadened to some extent, indicating that as Al atoms substitute for Si in the lattice the cubic environment of the Fe sites becomes somewhat distorted. Although the first NN environment remains cubic at an Fe(*B*) site, it does not at an Fe(*A*) or (*C*) site. Second NN environments will also change. In consequence of the imperfect cubic environment, the observed spectra will comprise a superposition of spectra representing slightly different isomer shifts and small quadrupole splittings, all essentially unresolved from one another. Examples of typical Mössbauer spectra are shown in Fig. 2.

The dependence on Al concentration  $x$  of the measured effective magnetic hyperfine field  $H_{\text{eff}}$  at the Fe(*B*) and (*A*,*C*) sites at room temperature ( $295 \pm 2$  K) is shown in Figs. 3 and 4, respectively. For maximum reliability the measurements of  $H_{\text{eff}}$  at the *B* site were repeated by using the region-of-interest (ROI) mode operation to scan only the outer two peaks of the  $\text{Fe}_3\text{Al}_x\text{Si}_{1-x}$  spectra. As the figures show, with increasing Al concentration  $H_{\text{eff}}$  of the *B* site decreases whereas that of the *A*, *C* sites increases. The  $^{57}\text{Fe}$  NMR spin-echo measurements on  $\text{Fe}_3\text{Al}_x\text{Si}_{1-x}$  ( $0 \leq x \leq 0.25$ ) showed  $H_{\text{eff}}$  to decrease at both the *B* and *A*, *C* sites. This dependence of  $H_{\text{eff}}$  at the *A*, *C* sites on Al concentration is opposite

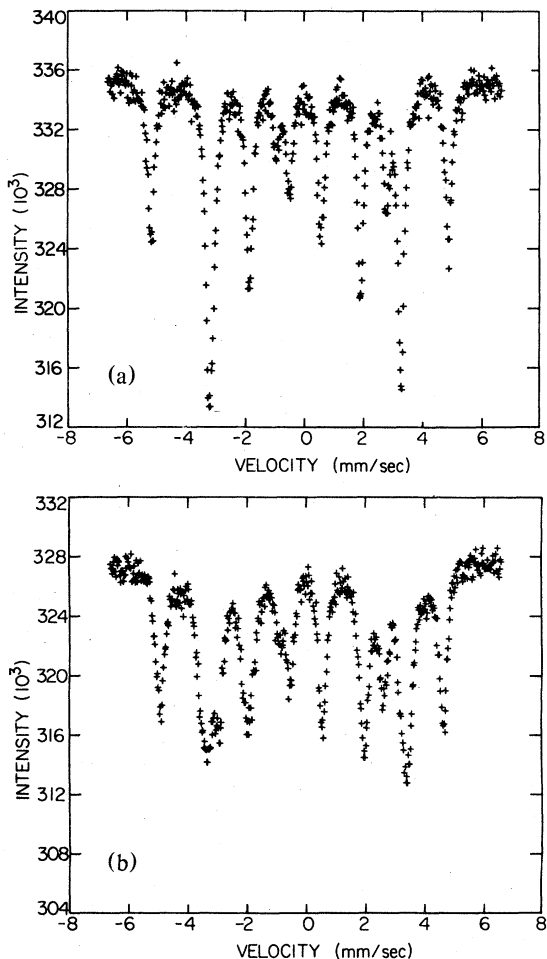


FIG. 2. (a) Mössbauer spectrum of  $\text{Fe}_3\text{Si}$  at  $T = 295.2$  K. (b) Mössbauer spectrum of  $\text{Fe}_3\text{Al}_{0.6}\text{Si}_{0.4}$  at  $T = 295.2$  K.

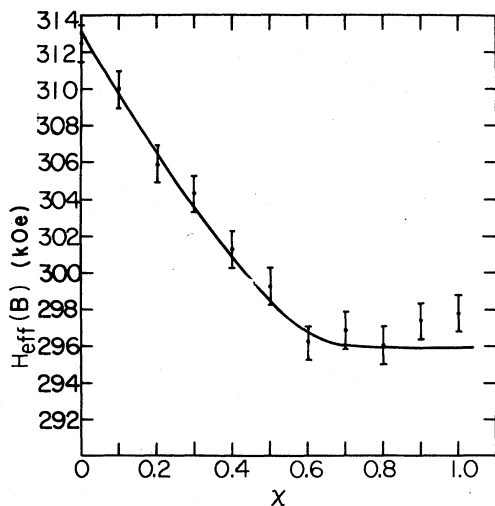


FIG. 3. Measured variation of the  $^{57}\text{Fe}$  effective magnetic hyperfine field with Al concentration  $x$  at the  $B$  site in  $\text{Fe}_3\text{Al}_x\text{Si}_{1-x}$  system.

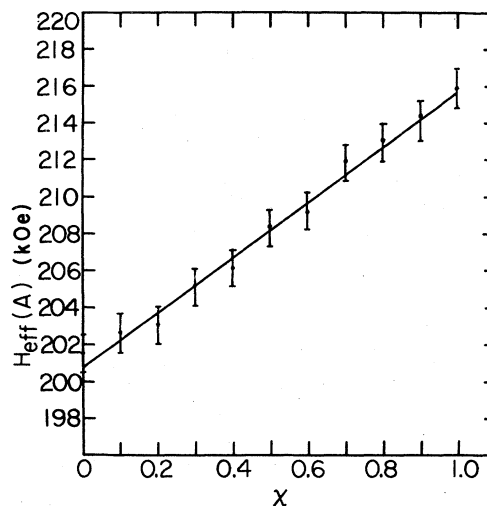


FIG. 4. Measured variation of the  $^{57}\text{Fe}$  effective magnetic hyperfine field with Al concentration  $x$  at  $A, C$  sites in  $\text{Fe}_3\text{Al}_x\text{Si}_{1-x}$  system.

to that reported here. Earlier Mössbauer-effect measurements<sup>4,10</sup> on  $\text{Fe}_3\text{Si}$  and  $\text{Fe}_3\text{Al}$  indicated clearly that  $H_{\text{eff}}$  at  $A, C$  sites in  $\text{Fe}_3\text{Al}$  is larger than that at  $A, C$  sites in  $\text{Fe}_3\text{Si}$ . Therefore, we expect the  $A, C$ -site  $H_{\text{eff}}$  to increase with increasing Al concentration  $x$  in the pseudobinary alloy system  $\text{Fe}_3\text{Al}_x\text{Si}_{1-x}$ . The isomer shifts,  $\delta$ , at the two sites are shown in Fig. 5 as functions of Al concentration. These shifts are in reference to the  $^{57}\text{Co}$  in Cu source which has in turn a shift of 0.214 mm/sec relative to Armco iron foil. Both isomer shifts decrease with increasing Al concentration, but at the  $B$  site the change levels off for the Al-rich alloys.

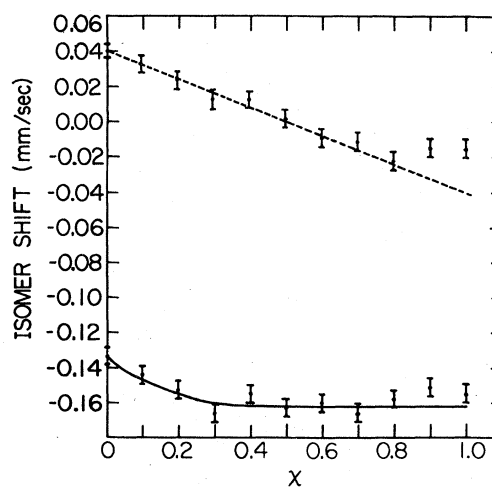


FIG. 5. Measured variation of the  $^{57}\text{Fe}$  isomer shift with Al concentration at  $B$  site (full line) and  $A, C$  sites (dashed line) in the  $\text{Fe}_3\text{Al}_x\text{Si}_{1-x}$  system.

## IV. DISCUSSION

## A. Effective magnetic hyperfine fields

For iron metal and its alloys in which the orbital angular momentum is quenched,  $H_{\text{eff}}$  at the iron atom results from the Fermi contact interaction between the nucleus and  $s$ -like conduction electrons. The Fermi contact interaction can be regarded as arising from contributions due to core polarization and to  $4s$ -like conduction-electron polarization. The core polarization contribution is large and negative. The contribution from the polarization of  $4s$ -like conduction electrons can be attributed to unpaired  $4s$  electrons and to paired bond electrons. In iron metal these yield only a small positive contribution.<sup>11</sup>

Both the symmetrized-augmented-plane-wave (SAPW) band structure calculation<sup>12</sup> for ordered  $\text{Fe}_3\text{Al}$  and the APW calculation<sup>9</sup> for ordered  $\text{Fe}_3\text{Si}$  showed that a large gap is opened up between bonding and antibonding states of iron  $s$  and aluminum (silicon)  $s$  electrons. The states in the gap are primarily of iron  $d$  and aluminum (silicon)  $p$  character. Furthermore, the Fermi energy  $E_F$  lies just across the  $d$  band, and the bonding  $s$  band falls far below  $E_F$ . In view of these results as well as the calculation<sup>12</sup> of the number of  $s$  character electrons inside and outside the APW sphere, we expect that there are very few unpaired  $4s$ -like electrons. And consequently, changes in  $H_{\text{eff}}$  due to these will be very small. The dominant factors responsible for changes in  $H_{\text{eff}}$  will be changes in polarization of core  $s$  electrons and of  $4s$ -like paired electrons by the magnetic moments in  $\text{Fe}_3\text{Al}_x\text{Si}_{1-x}$ . Thus, we expect that the observed behavior of  $H_{\text{eff}}$  reveals to a considerable extent the behavior of the magnetic moments in this system as  $x$  increases from 0 to 1.

The results of the  $\text{Fe}_3\text{Si}$  band-structure calculation<sup>9</sup> show that the total density-of-states (DOS) has five distinct peaks while the  $B$ -site component has only three and the  $d$  component of the  $A, C$  sites has four, one of which falls at a minimum of the  $B$  site DOS. Based on this result, and by postulating an exchange splitting consistent with the observed moments, Switendick found that the spin-down Fermi energy lies near a minimum (maximum) of the  $B$  site ( $A, C$  site) DOS, and that the spin-up Fermi energy lies at the point where the  $A, C$  density is much greater than the  $B$  site density. The major features of the band structure are that the states at  $E_F$  are predominantly associated with the  $A, C$  sites and that charge has been transferred from the  $B$  to the  $A, C$  sites. As Mn substitutes for Fe in  $\text{Fe}_3\text{Si}$ , charge transfer is reduced and exchange splitting decreased, consistent with the observed magnetic behavior.

In a rigid-band scheme, as Al substitutes for Si in  $\text{Fe}_3\text{Si}$  one electron is removed per substitution and the Si core is replaced by the Al core. Since near  $E_F$

most states belong to  $A, C$  sites, electrons are removed primarily from these. In addition, charge transfer from  $B$  to  $A, C$  sites will be reduced and the exchange splitting will be decreased. The results of Switendick's rigid-level calculation for  $\text{Fe}_3\text{Si}$  are shown in Fig. 6. In removing one electron (per formula unit) all the spin-up electrons in the antibonding  $\Gamma_{15}$  level are removed together with some from the  $\Gamma'_{12}$  level. Since due to admixture some of the  $\Gamma_{15}$  electrons are on  $B$  sites, the  $B$ -site moment is slightly reduced. The spin-down  $\Gamma'_{25}$  level is now too high, causing the exchange splitting to decrease and some electrons from the spin-down  $\Gamma'_{25}$  level to fill the spin-up  $\Gamma'_{12}$  level. Therefore, the  $A, C$  site moment will increase. This interpretation is consistent with the neutron diffraction measurement results,<sup>1-3</sup> i.e., the moment on the  $A, C$  sites is smaller in  $\text{Fe}_3\text{Si}$  than in  $\text{Fe}_3\text{Al}$ , and the moment on the  $B$  sites is greater in  $\text{Fe}_3\text{Si}$  than in  $\text{Fe}_3\text{Al}$ . For the  $\text{Fe}_3\text{Al}_x\text{Si}_{1-x}$  system we expect the moment on the  $A, C$  sites to increase and that on the  $B$  sites to decrease with increasing  $x$ . And in consequence, we expect the core polarization contribution to  $H_{\text{eff}}$  to follow the trend of the magnetic moments.

In fact, the Mössbauer  $H_{\text{eff}}$  data shown in Figs. 3 and 4 clearly follow this trend. Since the electrons removed from  $B$  sites as Al substitutes for Si are primarily up-spin having low DOS near  $E_F$  we expect to see the behavior of the  $B$ -site  $H_{\text{eff}}$  level off due to depletion of electrons before the full  $\text{Fe}_3\text{Al}$  composition is reached, as is indeed the case (Fig. 3). On the other hand, the increase in the moment and  $H_{\text{eff}}$  at  $A, C$  sites is due primarily to the removal of down-spin electrons which have a large DOS near  $E_F$ .

Hence,  $H_{\text{eff}}$  continues to increase uniformly right up

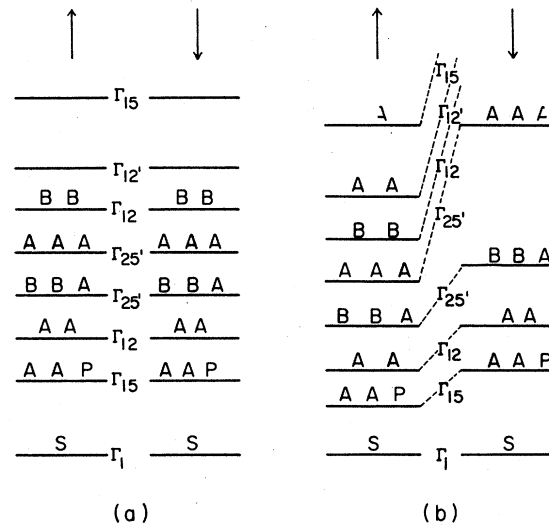


FIG. 6. (a) Rigid-level model for paramagnetic  $\text{Fe}_3\text{Si}$ . (b) Spin-split levels for  $\text{Fe}_3\text{Si}$  (from Ref. 9).

to Fe<sub>3</sub>Al (Fig. 4). The NMR spin-echo measurements<sup>8</sup> on Fe<sub>3</sub>Al<sub>x</sub>Si<sub>1-x</sub> ( $0 \leq x \leq 0.25$ ) showed a decrease of  $H_{\text{eff}}$  at both *B* and *A*, *C* sites, inconsistent with the present as well as previous<sup>4,10</sup> Mössbauer-effect measurements.

### B. Isomer shift

For Mössbauer absorber and source the isomer shift  $\delta$  is defined by

$$\delta = (2\pi/5)Ze^2(R_e^2 - R_g^2)[|\psi(0)|_a^2 - |\psi(0)|_s^2] \quad (1)$$

where  $R_e$  and  $R_g$  are the radii of the nuclear excited and ground states and  $|\psi(0)|_a^2$  and  $|\psi(0)|_s^2$  are the total *s*-like electron densities at the absorber and source, respectively. For a given source, the relative change in  $\delta$  in a series of different absorbers reflects the change in electron charge density at the absorber nuclei. Since for <sup>57</sup>Fe,  $R_e < R_g$ ,<sup>13</sup> a positive shift implies a decrease in electron density, and vice versa.

The measured isomer shifts for Fe<sub>3</sub>Al<sub>x</sub>Si<sub>1-x</sub> shown in Fig. 5 clearly indicate that the *A*, *C* sites have a positive shift relative to the *B* sites. This is the result of charge transfer from *B* to *A*, *C* sites due to the differences in local environment and bonding character at these sites. Whereas *B* sites have eight first-NN Fe atoms and six second-NN Si(Al) atoms. The Fe atoms in *A*, *C* sites have four Fe and four Si(Al) atoms as first NN and six second-NN Fe atoms. From the standpoint of local environment the strongly interacting Si(Al) *sp* band would produce a strong Fe-Si(Al) coupling at the *A*, *C* sites. Therefore, in the paramagnetic state the lower energy states will belong to the *A*, *C* sites, and the higher energy states will belong to *B* sites. Because spins at different sites experience different crystal potentials the result is an exchange splitting of the energy bands. The exchange energy is partially compensated by Coulomb energy via charge transfer from *B* to *A*, *C* sites. Thus the *A*, *C* sites must be more negative than *B* sites, and the shielding of *s*-like electrons by *3d* electrons will be more effective at *A*, *C* sites relative to that at *B* sites. Consequently, a more positive isomer shift is expected for the *A*, *C* sites relative to that at *B* sites, as is observed.

Since Al has one less electron than Si, as Al substitutes for Si in this system charge transfer is reduced and so is the exchange splitting. This results in reduced electron density at both *B* and *A*, *C* sites and in reduced shielding of *s*-like electrons. Therefore,  $\delta$  becomes negative as  $x$  increases. The strong similarity between the composition dependence of  $H_{\text{eff}}$  and of  $\delta$  at corresponding sites reinforces the correctness of the picture which qualitatively explains the behavior of  $H_{\text{eff}}$  at both sets of sites, namely, that the effect of Al substitution for Si reduces the up-spin electron density at *B* sites and the down-spin density at the *A*, *C* sites.

### C. Curie temperatures and temperature dependence of $H_{\text{eff}}$

The measured temperature dependence of  $H_{\text{eff}}$  at both *B* and *A*, *C* sites is shown in Fig. 7 in the form of plots of reduced  $H_{\text{eff}}$  values [i.e.,  $H_{\text{eff}}(T)/H_{\text{eff}}(0)$ ] versus reduced temperature,  $T/T_C$ , for four representative Al concentrations. Curie temperatures and  $H_{\text{eff}}(0)$  values are given in the figure caption. Similar measurements were made for all of the samples, and the dependence of the resulting Curie temperatures on Al concentration is shown in Fig. 8.

The reduced  $H_{\text{eff}}$  curves in Fig. 7 are essentially the same for both sites although the *B*-site curves decrease slightly less rapidly than those of the *A*, *C* sites. This behavior suggests that the exchange interaction between localized spins is long range because in the Heisenberg model with increasing temperature  $H_{\text{eff}}$  should decrease more rapidly at atoms near a nonmagnetic impurity. Mössbauer measurements<sup>14</sup> of Fe-4 at. % Si and Fe-4.3 at. % Al showed similar behavior, and from these results van der Woude and Sawatzky<sup>14</sup> obtained  $\mathcal{J}/N(E_F)J^2 = 0.015$  and concluded that itinerant exchange is more important than direct exchange. Here  $J$  and  $\mathcal{J}$  are coupling constants between itinerant-localized and localized-localized spins, respectively, in the phenomenological Hamiltonian<sup>15</sup>

$$H = H_0 - 2J \sum_i \vec{\sigma}(i) \cdot \vec{S}_i - 2\mathcal{J} \sum_{i < j} \vec{S}_i \cdot \vec{S}_j \quad (2)$$

where  $H_0$  includes the kinetic energy and mutual interactions between itinerant electrons,  $\vec{\sigma}(i)$  is an itinerant spin at site  $i$ , and  $\vec{S}_i$  is a localized spin. Van der Woude and Sawatzky<sup>14</sup> concluded that the exchange coupling felt by the magnetic moment of a particular iron atom is not disturbed by the presence of Si(Al) atoms in the alloys, and we conclude that the same situation occurs in the Fe<sub>3</sub>Al<sub>x</sub>Si<sub>1-x</sub> system.

The dependence of reduced  $H_{\text{eff}}$  on reduced temperature shown in Fig. 7 clearly indicates small differences in behavior for different Al concentrations. The curves decrease more rapidly with increasing Al content. In mean-field theory the magnetic moment is determined by the relationships<sup>15</sup>

$$M = (1 + \chi_i \gamma) m_p B_s(m_p H_M/kT) \quad (3)$$

and

$$H_M = (\gamma^2 \chi_i + \beta) m_p B_s(m_p H_M/kT) \quad (4)$$

where  $m_p B_s(m_p H_M/kT) = M_l$  is the localized moment,  $B_s$  is the Brillouin function and  $M_l = \chi_i \gamma M_i$  is the itinerant moment, with  $\chi_i$  being the itinerant part of the spins susceptibility. The coefficients of  $\beta$  and  $\gamma$  of Hasegawa's model<sup>16</sup> are related<sup>15</sup> to the coupling constants  $\mathcal{J}$  and  $J$  by

$$\gamma = J\lambda/2 \quad (5)$$

and

$$\beta = Z\mathcal{J}\lambda^2/2 \quad (6)$$

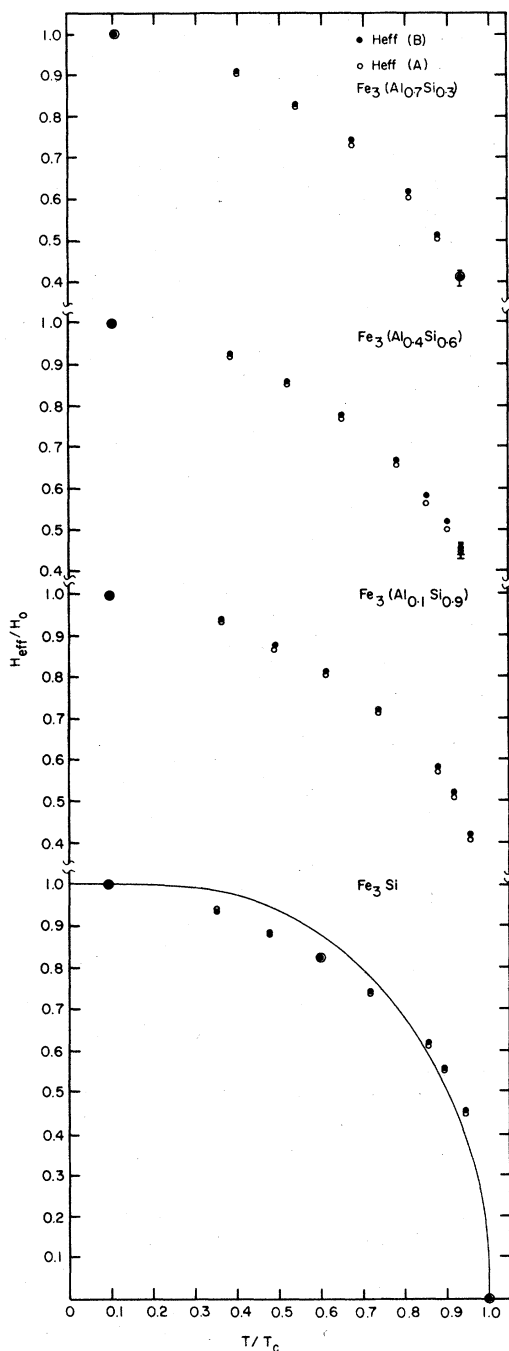


FIG. 7. Measured variation of the reduced effective magnetic hyperfine field with reduced temperature for the two sublattices of  $\text{Fe}_3\text{Al}_x\text{Si}_{1-x}$ . For  $x=0$ ,  $T_C = 838.2 \pm 2$  K,  $H_0(B) = 334.1$  kOe,  $H_0(A) = 214.4$  kOe; for  $x=0.1$ ,  $T_C = 816.2 \pm 2$  K,  $H_0(B) = 329.6$  kOe,  $H_0(A) = 217.1$  kOe; for  $x=0.4$ ,  $T_C = 769.2 \pm 2$  K,  $H_0(B) = 326.8$  kOe,  $H_0(A) = 224.1$  kOe; for  $x=0.7$ ,  $T_C = 744.2 \pm 2$  K,  $H_0(B) = 326.3$  kOe,  $H_0(A) = 233.8$  kOe. Full line is the  $S=1$  Brillouin function.

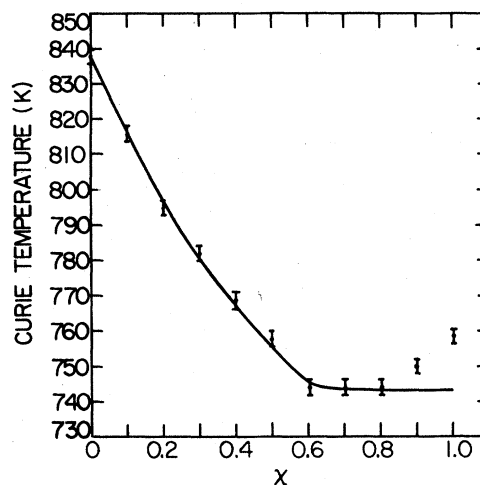


FIG. 8. Measured variation of the Curie temperature ( $T_C$ ) with Al concentration  $x$  in  $\text{Fe}_3\text{Al}_x\text{Si}_{1-x}$  system.

where  $Z$  is the number of nearest neighbors and  $\lambda = 2S/m_p$ . In this treatment, Hasegawa<sup>16</sup> considers the spin system in the paramagnetic state to be either one with zero moment on every site or one with moments  $\pm m_p$  on alternate sites. In the local moment situation as in iron, the paramagnetic state above  $T_C$  can be described approximately as a completely disordered alloy of local moments. Below  $T_C$  some fraction of the moments are correctly aligned.

Qualitatively, we expect that  $\chi_i\gamma$  will decrease with increasing Al concentration in the  $\text{Fe}_3\text{Al}_x\text{Si}_{1-x}$  system because Al contributes one less electron than Si and that changes in  $J$  and  $\mathcal{J}$  will be very small because neither Al nor Si possess magnetic moments. The slightly different temperature dependence of the reduced  $H_{\text{eff}}$  can thus be attributed to the decrease in  $\chi_i$  with increasing  $x$ .

The Brillouin function for  $S=1$  which is shown plotted in Fig. 7 lies above the experimental curves over an extended temperature range. To obtain a quantitatively satisfactory fit, the  $\chi_i\gamma$  value would need to be negative in the range of lower temperatures, implying that the itinerant-local coupling  $J$  is negative, i.e., antiferromagnetic.

The Curie temperature is determined by  $\beta$ ,  $\gamma$ , and  $\chi_i$  according to<sup>15</sup>

$$kT_C = \frac{1}{3} m_p^2 [(S+1)/S] (\gamma^2 \chi_i + \beta) \quad (7)$$

Since  $\chi_i$  is related to  $N(E_F)$ ,  $T_C$  is a function of  $J$ ,  $\mathcal{J}$ , and  $N(E_F)$ . As noted above, in the  $\text{Fe}_3\text{Al}_x\text{Si}_{1-x}$  system  $J$  and  $\mathcal{J}$  are essentially constant and independent of  $x$ . Within the rigid-band scheme,  $N(E_F)$  decreases as  $x$  increases. From Eq. (7)  $T_C$  will therefore decrease with increasing Al concentration. The measured dependence of  $T_C$  on Al concentration  $x$  shown in Fig. 8 agrees well with this expectation.

#### D. Properties of the Al-rich alloys

The rise in  $T_C$  seen in Fig. 8 and the increase in  $\delta$  of the  $A$ ,  $C$  sites (Fig. 5) and in  $H_{\text{eff}}$  of the  $B$  sites (Fig. 3) which occur in the Al-rich alloys are presumably the result of lattice disorder. Slowly cooled samples of  $\text{Fe}_3\text{Al}$  have been shown to contain a high density of antiphase boundaries are not completely ordered.<sup>7,8</sup> In fact, lattice parameter data in Ref. 7 for the  $\text{Fe}_3\text{Al}_x\text{Si}_{1-x}$  system indicate a slight negative deviation relative to the Vegard line. Associated with this increase in lattice parameter and destruction of long-range order is an increase in saturation moment.<sup>17</sup> This behavior is consistent with the magnetovolume effect which is associated locally with magnetized atoms. The increase in  $T_C$  in the Al-rich alloys due to disorder is consistent with the experimental results of magnetic moment and  $T_C$ .<sup>18</sup> Here, the moment and Curie temperature drop rapidly due to formation of the order  $DO_3$  structure.

#### V. CONCLUSION

Mössbauer-effect spectroscopy has been used to measure the temperature dependence of the  $^{57}\text{Fe}$  ef-

fective magnetic hyperfine field  $H_{\text{eff}}$  and isomer shift  $\delta$  across the entire  $\text{Fe}_3\text{Al}_x\text{Si}_{1-x}$  system ( $0 \leq x \leq 1$ ) from 77 K to the Curie temperature, the latter also being determined from these measurements. The observed dependence of  $H_{\text{eff}}$  and  $\delta$  on Al concentration can be qualitatively understood in terms of the calculated band structure of  $\text{Fe}_3\text{Si}$ . The changes in  $H_{\text{eff}}$  and  $\delta$  at the  $B$  sites with increasing Al concentration are due primarily to a decrease in the number of spin-up electrons at these sites, whereas the changes in  $H_{\text{eff}}$  and  $\delta$  at the  $A$ ,  $C$  sites result primarily from a decrease in the number of spin-down electrons at these sites.

#### ACKNOWLEDGMENTS

The authors express their appreciation of Professor F. X. Kayser for furnishing samples of his carefully characterized  $\text{Fe}_3\text{Al}_x\text{Si}_{1-x}$  alloys suitable for Mössbauer-effect study. Ames Laboratory is operated for the U.S. Department of Energy by Iowa State University under Contract No. W-7405-Eng-82. This research was supported by the Director of Energy Research, Office of Basic Energy Sciences, WPAS-KC-02-02-02.

- <sup>1</sup>R. Nathans, T. Pigott, and C. G. Shull, *J. Phys. Chem. Solids* **6**, 38 (1958).  
<sup>2</sup>S. J. Pickart and R. Nathans, *Phys. Rev.* **123**, 1163 (1961).  
<sup>3</sup>A. Paolette and L. Passari, *Nuovo Cimento* **32**, 25 (1964).  
<sup>4</sup>M. B. Stearns, *Phys. Rev.* **168**, 588 (1968).  
<sup>5</sup>V. Niculescu, K. Raj, J. I. Budnick, T. J. Burch, W. A. Hines, and A. H. Menotti, *Phys. Rev. B* **14**, 4160 (1976).  
<sup>6</sup>R. Haydock and M. V. You, *Solid State Commun.* **33**, 299 (1980).  
<sup>7</sup>J. G. Cowdery and F. X. Kayser, *Mater. Res. Bull.* **14**, 91 (1979).  
<sup>8</sup>V. Niculescu, K. Raj, T. Burch, and J. I. Budnick, *J. Phys. F* **7**, L73 (1977).  
<sup>9</sup>A. C. Switendick, *Solid State Commun.* **19**, 511 (1976).  
<sup>10</sup>C. E. Johnson, M. S. Ridout, and T. E. Cranshaw, *Proc.*

- Phys. Soc. London* **81**, 1079 (1963).  
<sup>11</sup>K. J. Duff and T. P. Das, *Phys. Rev. B* **3**, 192 (1971).  
<sup>12</sup>S. Ishida, J. Ishida, S. Asano, and J. Yamashita, *J. Phys. Soc. Jpn.* **41**, 1570 (1976).  
<sup>13</sup>L. R. Walker, G. K. Wertheim, and V. Jaccarino, *Phys. Rev. Lett.* **6**, 98 (1961).  
<sup>14</sup>F. van der Woude and G. A. Sawatzky, *Phys. Rep.* **12C**, 335 (1974).  
<sup>15</sup>D. M. Edwards, *J. Magn. Magn. Mater.* **15-18**, 262 (1980).  
<sup>16</sup>H. Hasegawa, *J. Phys. Soc. Jpn.* **46**, 1504 (1979).  
<sup>17</sup>A. Taylor and R. M. Jones, *J. Phys. Chem. Solids* **6**, 16 (1958).  
<sup>18</sup>M. Fallot, *Ann. Phys. (Paris)* **6**, 305 (1936).